Fachtagung "Lasermethoden in der Strömungsmesstechnik"
7. – 9. September 2004, Universität Karlsruhe

Wind Load Coefficients for Pyramidal Buildings

M. Ikhwan & B. Ruck
Laboratory of Building- and Environmental Aerodynamics
Institute for Hydromechanics
Kaiserstr. 12, 76128 Karlsruhe

Abstract

This study presents experimental investigations on flow and pressure characteristics around pyramidal buildings. The experiments were conducted in an atmospheric boundary layer wind tunnel at the laboratory of building- and environmental aerodynamics, Institute for Hydromechanics, University of Karlsruhe. The flow velocities around the pyramids were measured using 2D Laser Doppler Anemometry (LDA). The pressure distributions on the pyramid surfaces were measured using a standard pressure tapping technique. Previous studies of pyramidal buildings showed that the pyramid base angle and wind direction are the most important parameters influencing the flow and pressure characteristics around pyramidal buildings. In this paper, additionally, the influence of the Jensen number is investigated. The obtained force (drag, lift) and moment coefficients for pyramidal buildings are described as a function of the aforementioned parameters.

1. Introduction

From the aerodynamic engineering point of view, the pyramidal building possesses its own interesting characteristics. The pyramidal geometry shows specific fluid mechanical properties when compared to other e.g. rectangular, sharp-edged configurations. This is mainly due the vertical wall taper.

Although the flow around pyramidal and rectangular buildings have some similarities [Chyu et al 1996, Peterka et al 1985], the vortex regime especially in the downstream or wake region is very different. Fig. 1 shows sketches of the flow structure around a pyramid, which are depicted from previous studies [Abuomar et al 2000, Ikhwan et al 2003, 2004, Peterka et al 1985, Roth 1997] . It can be inferred from Fig. 1(a) that the flow around a pyramid gives rise to a discrete horseshoe vortex system, which is similar in almost all bluff body flows. However, the vortex system attached to the pyramids are not so uniform as systems of rectangular bluff bodies. The wall taper induces a vortex system consisting of two conical vortices rotating near the outer edges of the leeward surface and a rotor vortex in the vertical middle plane. The diameters of the two outer vortices depend on local pressure and height z. Thus, the aerodynamic loading of the structures is rather specific. Fig. 1(b) shows a flow visualization at the upstream edge near the bottom of the pyramid. It is shown that on the side walls at the upstream edge of the pyramid flow separation (A) and a vertical vortex system (B) occur.

The technical layout of pyramids with respect to wind load assumptions is usually not listed in standard tables. The Building Research Establishment (BRE), e.g., gives design values of the pressure coefficient (c_p) at different wind directions in the case of pyramid base angle ζ=45° [Cook 1985], where the angle is defined as the angle of surface declination of the pyramid. Unfortunately, this report does not cover investigations of pyramidal buildings for other base angles. These facts underline the need of systematic experimental investigations of pyramidal buildings, which today undergo a renaissance in architecture.

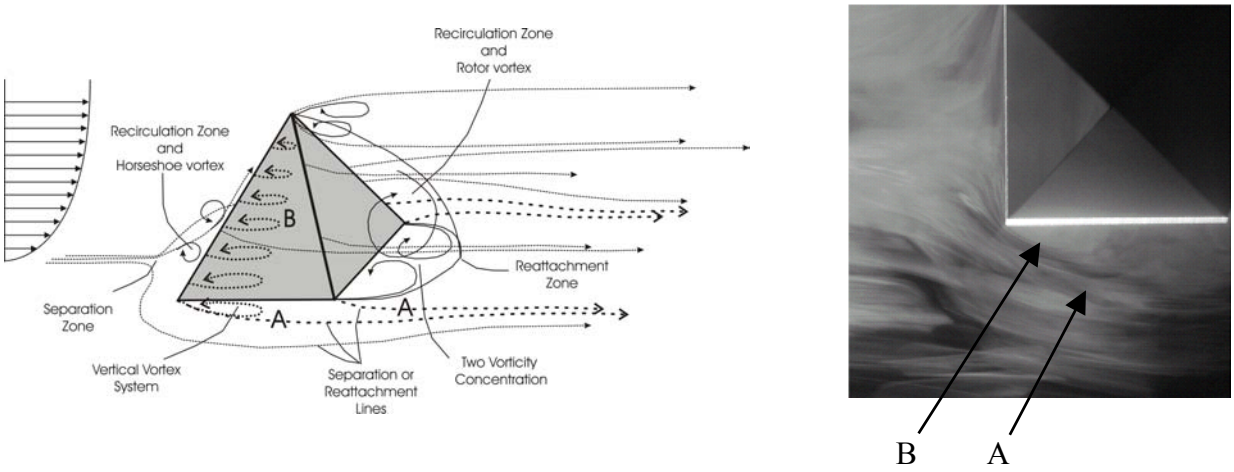

(a) 3D flow structure [Ikhwan et al 2004]

(b) flow visualization

Figure 1. Flow structure around a pyramid

In a previous study [Ikhwan et al 2003], it was shown that the variation of pyramid base angle and wind direction induce the most differences in the flow and pressure characteristics around pyramidal buildings. In this paper, the results of four additional pyramids with variation in base angle were added, so that in total 8 pyramids (ζ=20°, 30°, 40°, 45° 50°, 55°, 60°, and 70°) have been investigated. All of them have the same base area (length, l x l = 200 mm x 200 mm). In order to investigate the influence of the ratio of body height/roughness length, h/z_0, the Jensen number was varied in an additional experiment, where two pyramids of different height but with the same base angle (70°) were measured (base area 200 mm x 200 mm and 73 mm x 73 mm).

2. Experimental Setup

The experiments were carried out in the closed-loop 29 m long atmospheric boundary layer wind tunnel at the Laboratory of Building- and Environmental Aerodynamics, Institute for Hydromechanics, University of Karlsruhe. Longitudinal and vertical velocities were measured with the aid of a 2D Laser Doppler Anemometer (2D-LDA), working in forward light scattering mode using blue (488.0 nm) and green (514.5 nm) light from a 4 watts argon-ion laser, see Fig. 2. The scattered light signals were detected by photomultipliers and filtered from 300 KHz to 1 MHz. These filtered signals were processed using two counter-based signal processor TSI model IFA 550, which measures the time required for 11 cycles of each Doppler burst. 1,2-propandiol droplets were generated with an evaporation-/condensation-type particle generator, producing seeding particles of 1.5 µm mean diameter.

The pressure distributions on the pyramid surfaces were measured using the standard pressure tapping technique. Pressure taps with 1.5 mm diameter were distributed systematically

on one half of a pyramid surface. The pyramid versions investigated were equipped with different numbers of pressure taps ranging from 46 to 59 due to different sizes in surface area.

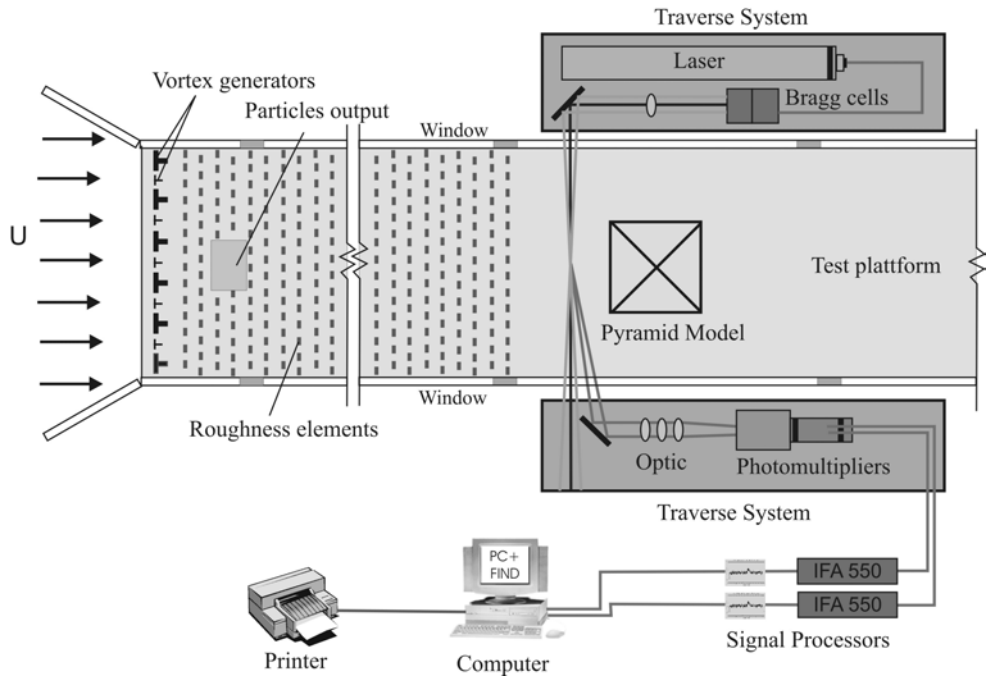

Figure 2. Sketch of the experimental set-up and flow data processing

Fig. 3 shows the mean wind velocity profile at two positions (upstream and downstream) in the test section of the wind tunnel. The profile indicated as 'upstream flow' is measured at 2.6 m behind the flow inlet in the test section - the starting point for the measuring section. The end point of the measuring section is located 0.8 m downstream from this starting point and the measured profile is indicated in Fig. 3 as 'downstream flow'. The velocity profiles are well fitted with α = 0.26 using the exponential velocity profile law. According to Plate [Plate 1995] and others the profile exponent can be categorized due to the dominating surface roughness (e.g. suburban or industrial area and city centres). See [Ikhwan et al, 2002, 2003, 2004] for more detail on the experimental set up and the characteristics of simulated boundary layer flow.

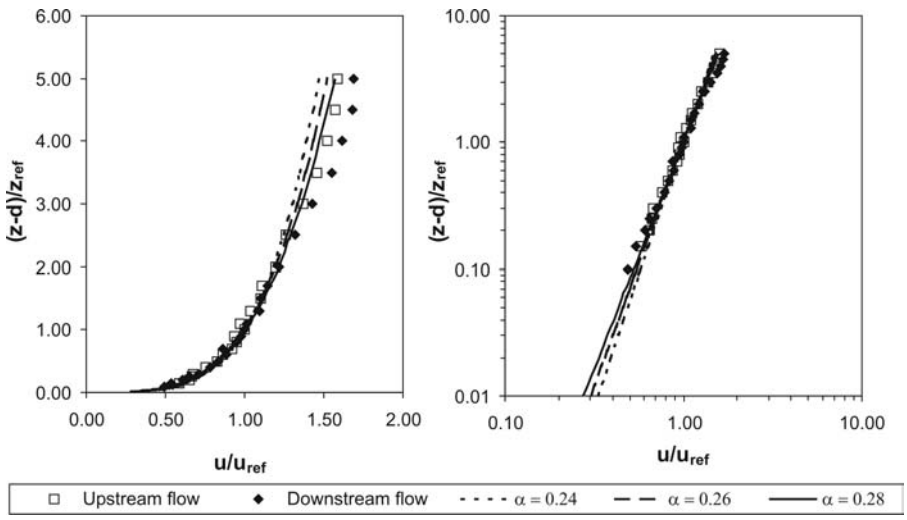

Figure 3. The variation of mean wind velocities with height [Ikhwan et al 2004]

3. Flow Characteristics

All flow fields were investigated with a wind direction of $\alpha' = 0°$ (wind normal to the front surface of the pyramid). The flow fields were measured ranging from l x l upstream to 2 x l downstream (l: length of the pyramid) of the pyramid and within a height from z=0 to z=1.5 x h_{70} (height of pyramid P70).

Velocity vector fields at the centre line cross-section (y/l =0) are shown in Fig. 4. From the plots given, the formation of recirculation zones in the lee of the pyramids can be observed. For pyramid P20, no recirculation zone is found (Fig. 4 (a)). This is due to the fact that the heights of pyramid P20 is really small (h20=36.40 mm) and the flow field is blended with the roughness element flow field. However the pattern shows that the velocities in the lee are still decreasing, also see [Ikhwan et al 2003].

A small recirculation zone can be observed in the lee of pyramid P30 (Fig. 4 (b)). This recirculation zone is attached to the backward facing pyramid surface. For pyramid with base angle > 45° (Fig. 4 (c) – (h)), which can be categorized as a tall building, 2h/l >1, the recirculation zone can be clearer visualized. The size of the recirculation zone increases with increasing base angle. The vector plots of the flow velocity reveal in this zone a large-scale fluid rotation. This large scale vortex is considered to be very stable in comparison to recirculation bubbles behind rectangular bluff bodies where the flapping of the shear layer intermittently causes the recirculation bubble to be convected downstream [Abuomar et al 2000]. Moreover, the recirculation zone in the lee of a pyramid is much shorter in length than that of a rectangular bluff body for similar height. As a consequence, the rotating mass must be smaller. Due to a smaller gradient between ambient pressure and back pressure of the pyramid, also the rotating velocity within the recirculation is decreased. The stability of the vortex system might come from the two very stable side vortices on the side walls and of the two very stable vortices at the corners of the backside of the pyramid. All of these vortices are found to have varying size and rotating velocity with height.

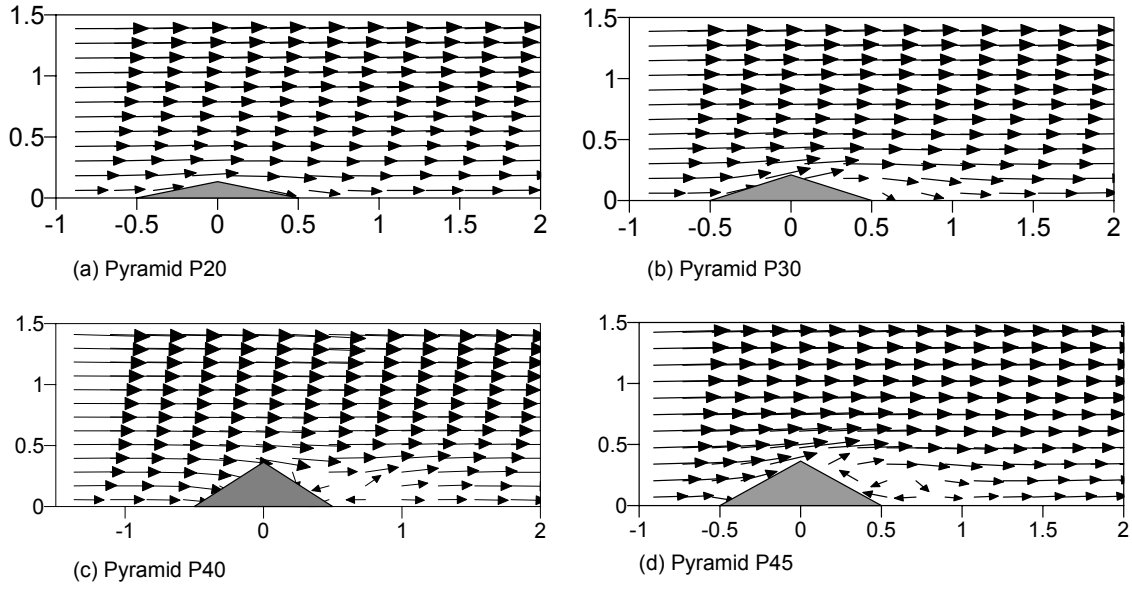

Figure 4 (a) – (d). Velocity vector fields at the center line cross section (y/l=0) of pyramids ($\alpha' = 0°$, u_∞ = 5 m/s, h_{70} = 274.7 mm)

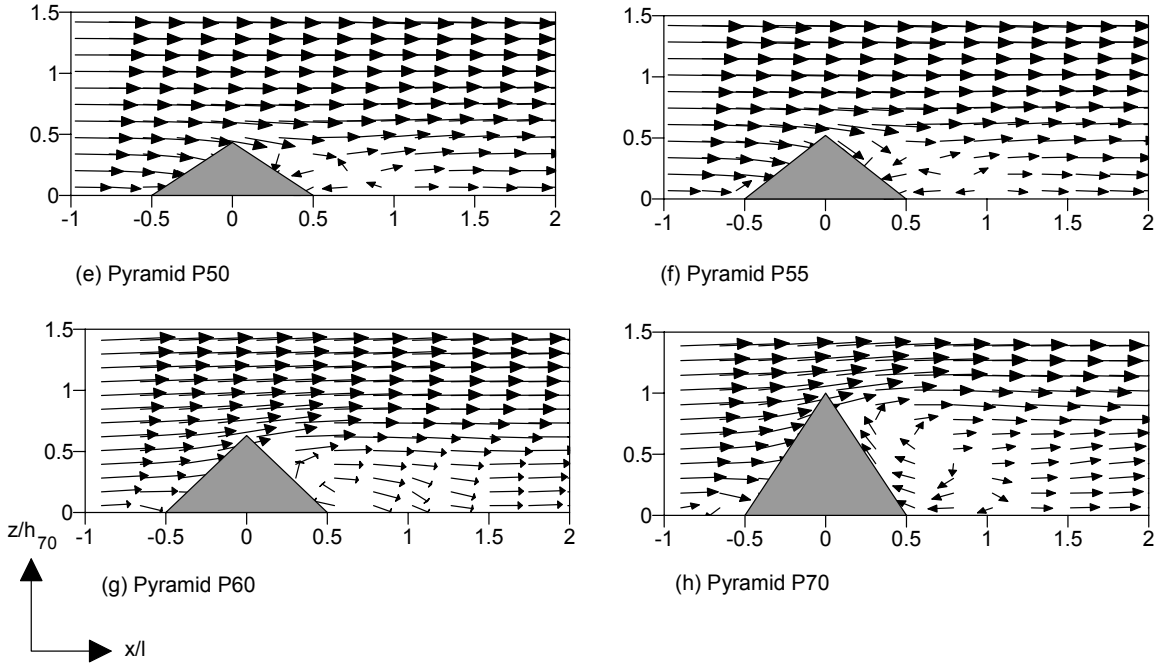

Figure 4 (e) – (h). Velocity vector fields at the center line cross section (y/l=0) of pyramids (α'= 0°, u_∞ = 5 m/s, h_{70} = 274.7 mm)

4. Force and Moment Coefficients

Pressure measurements were carried out with a velocity of 12 m/s in order to obtain measurable and reliable pressure differences. Thirteen different wind directions (α') ranging from 0° to 180° with 15° increments for each pyramid were investigated. The distribution of normal pressure and fluctuations on the pyramid surfaces can be seen in previous studies [Ikhwan et all 2002, 2003, 2004, Peterka et al 1985]. In this paper, results of wind-induced forces are presented, deduced from an integration of local measured pressure values over the pyramid surfaces. Force is a vector quantity having an magnitude and a direction and a point of application in the three dimensions of space. This requires the coordinate axes convention to be defined, see table 1. The horizontal axes are aligned in the in-wind direction. The force in-wind is called drag force F_d, and force perpendicular to in-wind is called lift force, F_l. The forces are rendered dimensionless and expressed in terms of dimensionless coefficient, as can be seen in table 1.

Fig. 5(a) presents the drag coefficient (c_d) for five pyramids as a function of wind direction. The figure simply shows that greater base angle will have greater c_d. The different curves of drag coefficients vary in the same way for changing wind direction. The minimum c_d occurs at wind direction (α') 0° and 90°. The maximum occurs at α'= 15° and 75°. These mirror effects occur due to the symmetrical shape of the pyramid. In Fig. 5(b) it can be seen in an other plot that at wind direction 0° the drag coefficients are minimum.

Table 1. Force coefficients

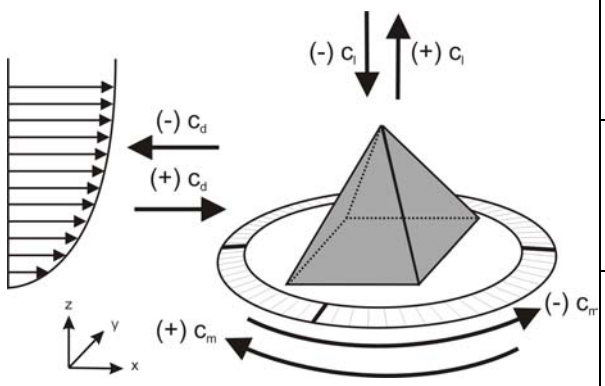	Drag coefficient	$c_d = \frac{F_d}{\frac{1}{2}\rho u_{ref}^2 A}$	(1)
	Lift coefficient	$c_l = \frac{F_l}{\frac{1}{2}\rho u_{ref}^2 A}$	(2)
	Moment coefficient	$c_{m-z} = \frac{M_z}{\frac{1}{2}\rho u_{ref}^2 A.l}$	(3)
½ ρu_{ref}^2 = reference dynamic pressure at the tip of pyramid, F_d is a drag force, F_l is a lift force, M_z is a moment working at z-axes, A is the projection area of the pyramid in wind direction, and l is the base length of the pyramid			

Another important parameter in atmospheric boundary layer flow is the Jensen number. This parameter expresses the heigt of the body divided by the roughness length (z_0=2.82 mm) of the surface, h/z_0, (Jensen, 1958). Typical Jensen number are between 50~500, however BRE suggests that the Jensen number in the range of 20~1000 will cover the range of real buildings [Cook 1985]. As stated in the introduction, in order to see how the Jensen number affects the force and moment coefficient, another pyramid model with base angle 70° were added. This model is denoted as pyramid P70b (ζ=70°, height:h= 100 mm, base length:l=73mm). In Fig. 5 (c) the drag coefficients of pyramid P70 (Je=110) and P70b (Je=40) are given as a function of wind direction. Again, the same distribution pattern of the drag coefficients against the wind directions can be observed for all pyramids. However, the magnitude of the drag coefficients between pyramid P70 and P70b are different. The drag coefficients for pyramid P70b decrease more than 30% when compared to pyramid P70. This indicates that the Jensen number can play a significant role in determining the magnitude of drag coefficients. Further investigations with respect to the influence of the Jensen number are in progress.

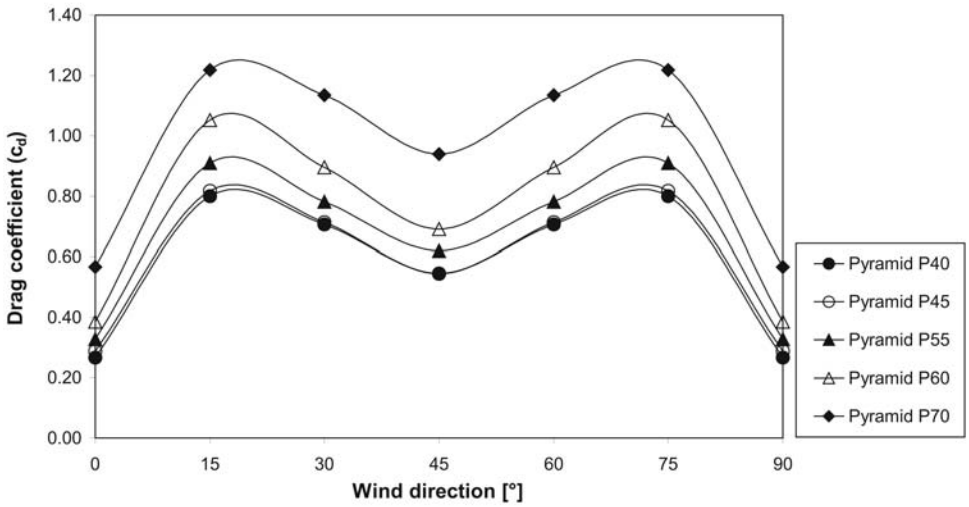

Figure 5(a). Drag coefficient (c_d) as a function of wind direction

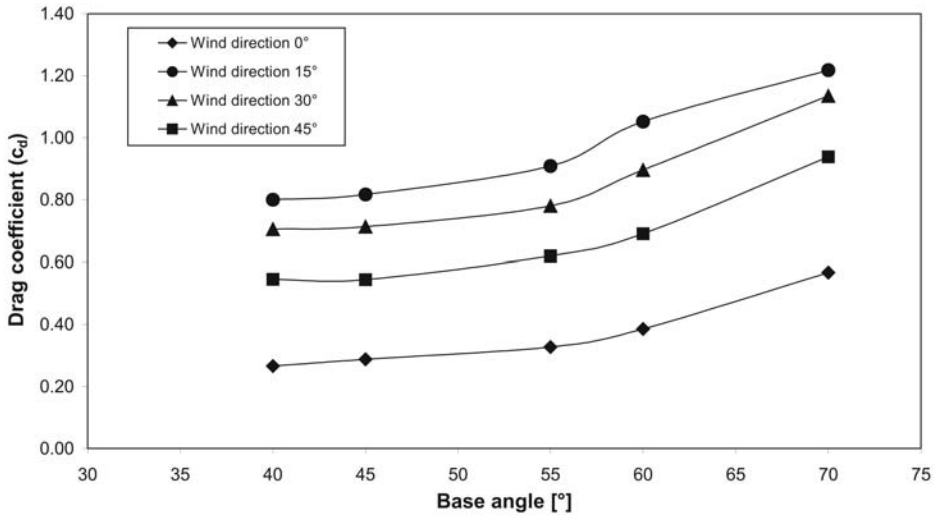

Figure 5(b). Drag coefficient (c_d) as a function of base angle

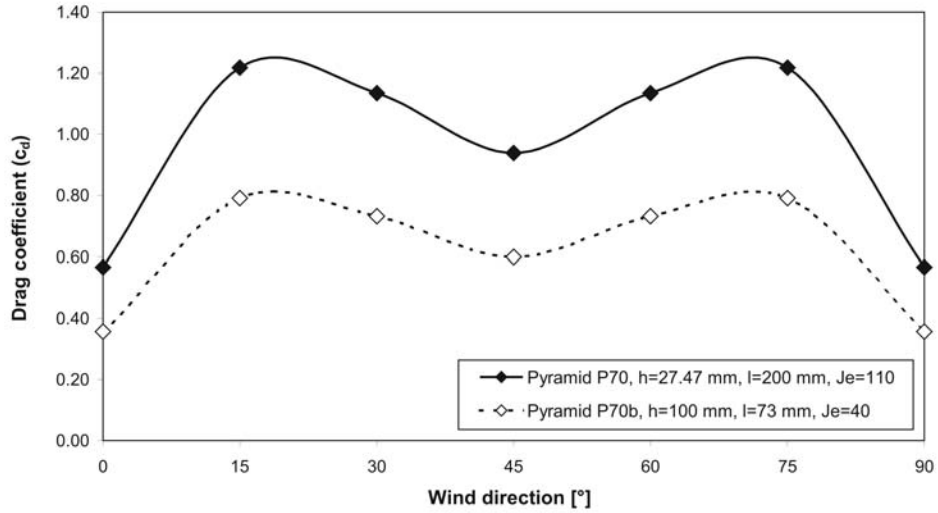

Figure 5(c). Drag coefficient (c_d) as a function of wind direction for pyramid P70 and P70b

Fig. 6(a), 6(b) and 6(c) show the lift coefficient for the pyramids investigated. In fig 6(a), the influence of a variation of wind direction on the lift coefficient can be observed. It can be inferred that two different curve types exist. Pyramid P40 and P45 show a similar dependency, whereas pyramid P55, P60 and P70 deliver somewhat different curves. It can be seen also that for pyramid P40 and P45 the dependency of wind direction is relatively small when compared to the other pyramids. In the previous study [Ikhwan et al, 2002, 2003], it was suggest that pyramidal buildings can be categorized as “shallow” and “steep” pyramid. This categorisation is underlined by the new results and also the results from Fig. 6(b) support this conclusion. The gradient of the curve of the lift coefficient is changing after a pyramid base angle of 55°.

In Fig. 6(c), the lift coefficient for pyramid P70 and P70b is given as a function of wind direction. The curves show a similar trend but the magnitude is different. The lift coefficient for steep pyramids increases significantly when the height of the pyramid with the same base angle (i.e. 70°) decreases. This underlines again the importance of the Jensen number for such experiments.

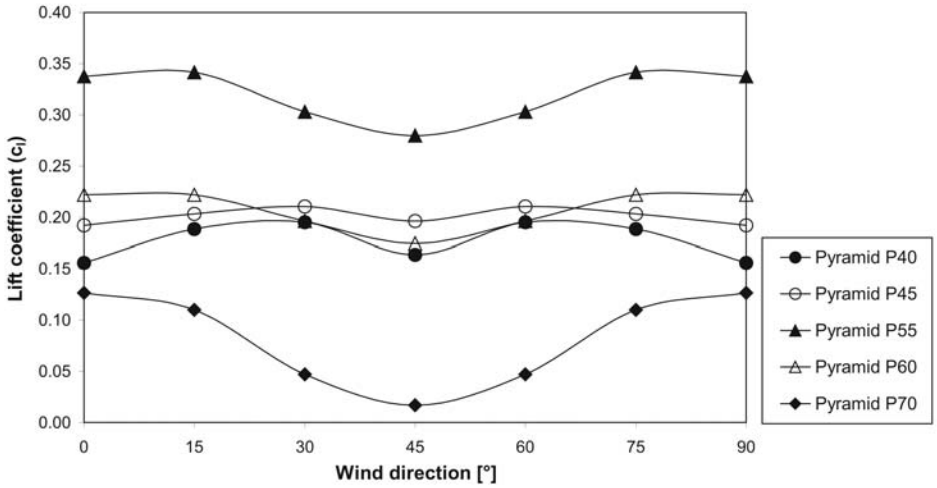

Figure 6(a). Lift coefficient (c_l) as a function of wind direction

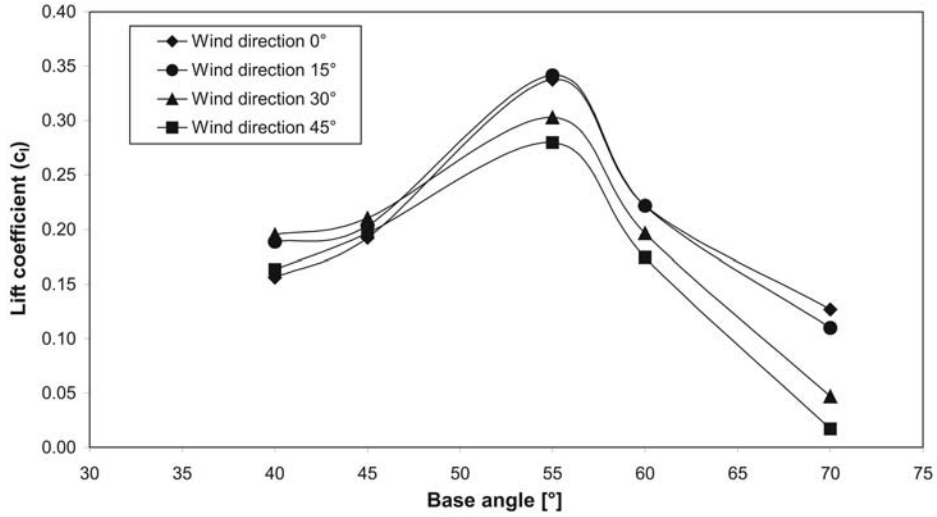

Figure 6(b). Lift coefficient (c_l) as a function of base angle

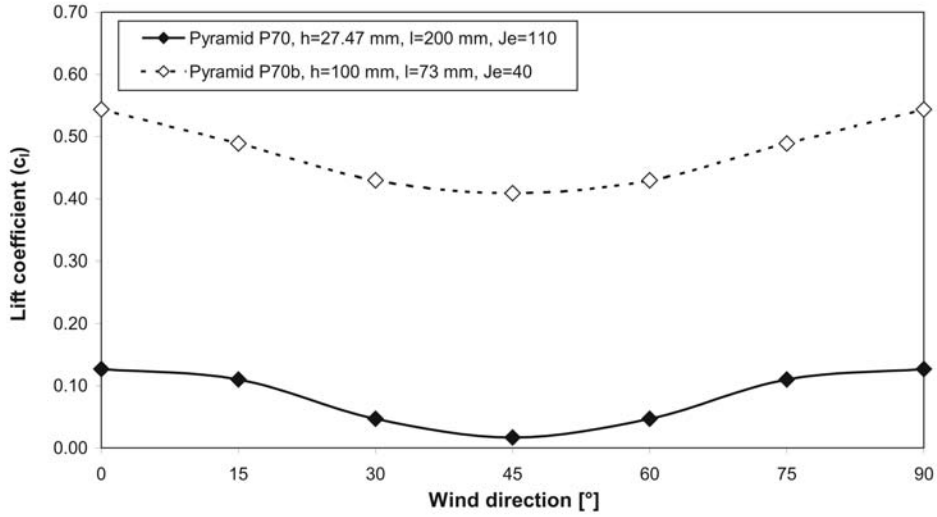

Figure 6(c). Lift coefficient (c_l) as a function of wind direction for pyramid P70 and P70b

Fig. 7(a), 7(b) and 7(c), show the moment coefficients accounting for moments only working at z-axes. The results show that the values of the moment coefficients are relatively small. Typical values are in the range of –0.025 to 0.025 (which is in a similar range to rectangular buildings) [Akins et al 1977]. However what is most interesting is the fact that different pyramid base angle can create different direction of rotation, as can be seen in Fig. 7(a) and 7(b). The moments of pyramids with base angles below 55° rotate in an other direction than those with base angles above 60°. This reversal of moment direction was never detected before.

The moment coefficients of pyramid P70 and P70b can be seen in Fig. 7(c) as a function of wind direction. The magnitude of the moment coefficient decrease as the height of the pyramid decreases. However, the direction of the moment remains the same. The results seem to show that the variation of base angle has a greater influence on the moment for pyramidal buildings than the height. However, at this paper, only one set of pyramids with the same base angle but different heights was investigated. More variations are required to conclude the interaction of both parameters.

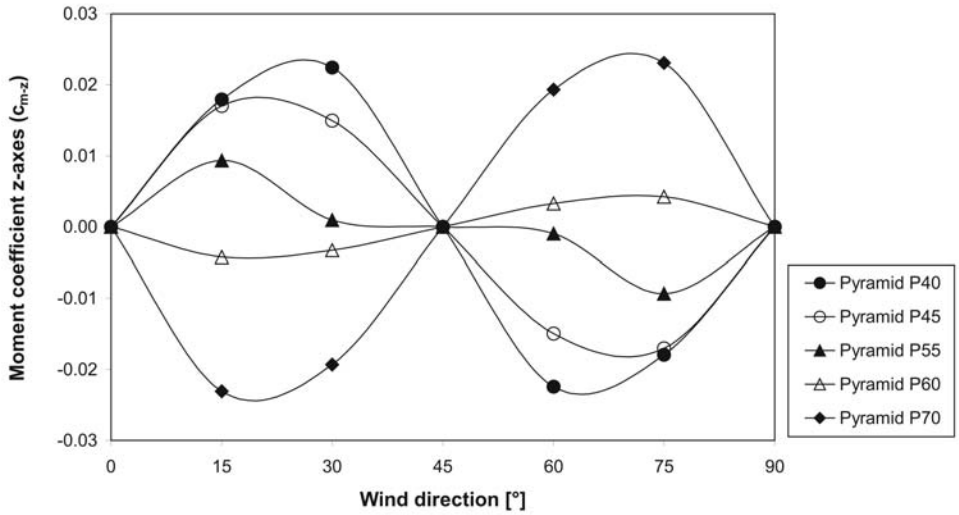

Figure 7(a). Moment coefficient (c_{m-z}) as a function of wind direction

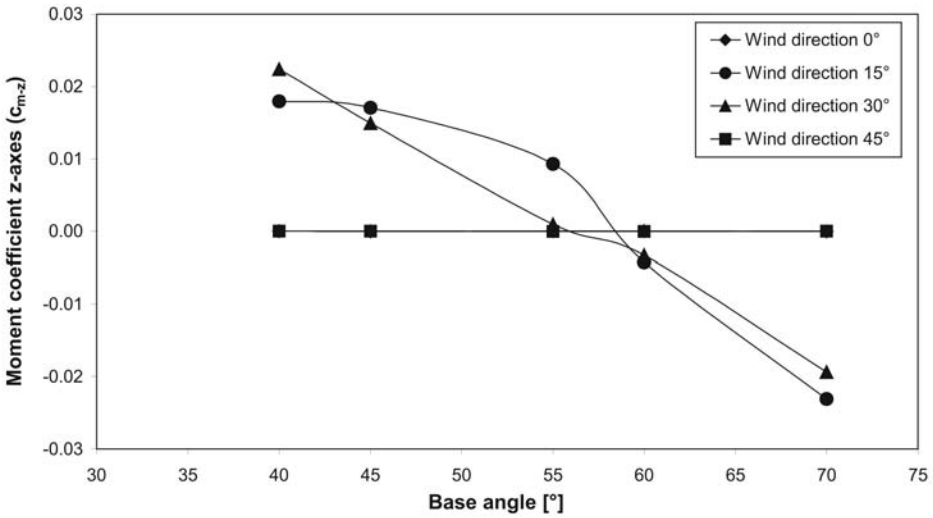

Figure 7(b). Moment coefficient (c_{m-z}) as a function of base angle

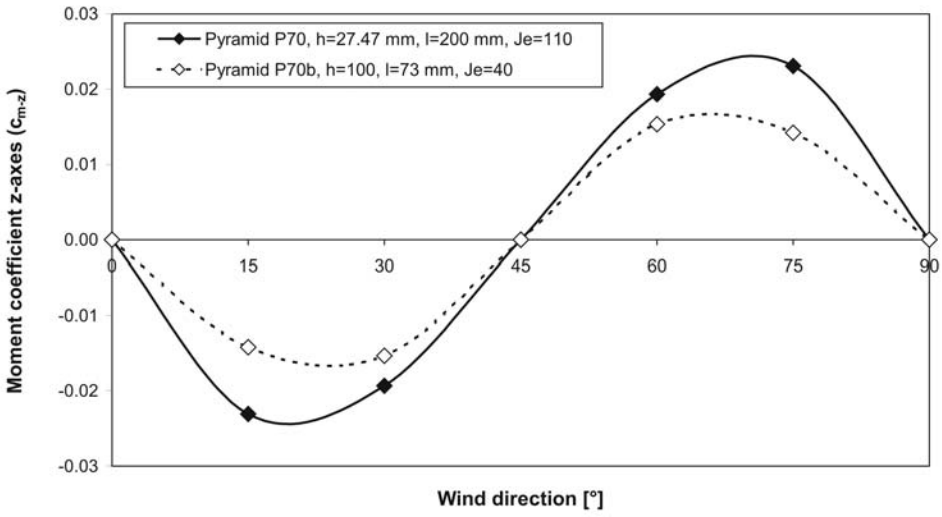

Figure 7(c). Moment coefficient (c_{m-z}) as a function of wind direction for pyramid P70 and P70b

5. Acknowledgements

The financial support of the Deutsche Forschungsgemeinschaft DFG/Bonn within the project No. Ru 345/25 is gratefully acknowledged by the authors.

6. Literature

Abuomar, M.M., Martinuzzi, R.J., 2000, An Experimental Investigation of the flow around a Surface Mounted Pyramid, 6th Triennial International symposium on Fluid Control, Measurement and Visualization, August 13-17, 2000, Sherbroke, Canada.

Akins, R.E., Peterka, J.A.,1977, Mean Force and Moment Coefficients for Buildings in Turbulent Boundary Layer, Journal of Industrial Aerodynamics,2 (1977), p.195-209.

Chyu, M.K., Natarajan, V., 1996, Heat Transfer on the Base of Three Dimensional Protruding Elements, Int. Journal of Heat Mass Transfer, Vol. 39, No.14 (1996), p. 2925-2935

Cook, N.J., 1985, The Designer's Guide to Wind Loading of Building Structures, Building Research Establishment Report, London, Butterworths.

Ikhwan, M., Ruck, B., 2004, Flow and Pressure Field Characteristics around Pyramidal Buildings. Submitted to Journal of Wind Engineering and Environmental Aerodynamics, February 2004.

Ikhwan, M., Ruck, B., 2003, Investigation of Flow and Pressure Phenomena around Pyramidal Structures, Proc.Physmod, Int. Workshop on Physical Modelling of Flow and Dispersion Phenomena. Sept., 2003, Prato-Italy.

Ikhwan, M., Ruck, B., 2003, Instationarität des Strömungs- und Druckfeldes bei der Pyramidenumströmung, Proceeding 11th GALA-Conference, *Lasermethoden in der Strömungmeßtechnik*, PTB, Braunschweig, September.

Ikhwan, M., Ruck, B., 2002, Investigation of Flow and Pressure Characteristics Around Pyramidal Shape Buildings, Proceeding 10th GALA-Conference, *Lasermethoden in der Strömungmeßtechnik*, University of Rostock, Germany, September.

Peterka, J.A., Meroney, R.N., Kothari, K.M., 1985, Wind Flow Patterns About Buildings. J. Wind Eng. Ind. Aerodyn. 21 (1985), p. 21-38.

Plate. E.J. (Ed.), 1995, *Windprobleme in dichtbesiedelten Gebieten WTG-Berichte Nr. 3*, Windtechnologische Gesellschaft e.V.

Roth, M., 1997, *Analyse der Umströmung pyramidenförmiger Hindernisse*, Diplomarbeit, IfH, Forschungsgruppe Stömungsmeßtechnik, Univ.Karlsruhe (TH).